

## Effects of O<sub>2</sub>, Ar, and H<sub>2</sub> gases on the field-emission properties of single-walled and multiwalled carbon nanotubes

A. Wadhawan, R. E. Stallcup, K. F. Stephens, J. M. Perez, and I. A. Akwani

Citation: *Appl. Phys. Lett.* **79**, 1867 (2001); doi: 10.1063/1.1401785

View online: <http://dx.doi.org/10.1063/1.1401785>

View Table of Contents: <http://apl.aip.org/resource/1/APPLAB/v79/i12>

Published by the [American Institute of Physics](http://www.aip.org).

---

### Related Articles

Breakdown voltage reliability improvement in gas-discharge tube surge protectors employing graphite field emitters

*J. Appl. Phys.* **111**, 083301 (2012)

Effect of sputtered lanthanum hexaboride film thickness on field emission from metallic knife edge cathodes

*J. Appl. Phys.* **111**, 063717 (2012)

Space charge and quantum effects on electron emission

*J. Appl. Phys.* **111**, 054917 (2012)

Enhanced electron field emission from plasma-nitrogenated carbon nanotips

*J. Appl. Phys.* **111**, 044317 (2012)

Field-emission properties of individual GaN nanowires grown by chemical vapor deposition

*J. Appl. Phys.* **111**, 044308 (2012)

---

### Additional information on *Appl. Phys. Lett.*

Journal Homepage: <http://apl.aip.org/>

Journal Information: [http://apl.aip.org/about/about\\_the\\_journal](http://apl.aip.org/about/about_the_journal)

Top downloads: [http://apl.aip.org/features/most\\_downloaded](http://apl.aip.org/features/most_downloaded)

Information for Authors: <http://apl.aip.org/authors>

## ADVERTISEMENT



ACCELERATE AMBER AND NAMD BY 5X.  
TRY IT ON A FREE, REMOTELY-HOSTED CLUSTER.

LEARN MORE

## Effects of O<sub>2</sub>, Ar, and H<sub>2</sub> gases on the field-emission properties of single-walled and multiwalled carbon nanotubes

A. Wadhawan, R. E. Stallcup II, K. F. Stephens II, and J. M. Perez<sup>a)</sup>  
*Department of Physics, University of North Texas, Denton, Texas 76203*

I. A. Akwani  
*Corning, Inc., Science and Technology Division, Corning, New York 14831*

(Received 15 May 2001; accepted for publication 20 July 2001)

We compare the effects of O<sub>2</sub>, Ar, and H<sub>2</sub> gases on the field-emission (FE) properties of single-walled carbon nanotubes (SWNTs) and multiwalled carbon nanotubes (MWNTs). We find that H<sub>2</sub> and Ar gases do not significantly affect the FE properties of SWNTs or MWNTs. O<sub>2</sub> temporarily reduces the FE current and increases the turn-on voltage of SWNTs. Full recovery of these properties occurs after operation in UHV. The higher operating voltages in an O<sub>2</sub> environment cause a permanent decrease of the FE current and an increase in the turn-on field of MWNTs. The ratios of the slopes before and after O<sub>2</sub> exposure are approximately 1.04 and 0.82 for SWNTs and MWNTs, respectively. © 2001 American Institute of Physics. [DOI: 10.1063/1.1401785]

Considerable interest has been shown of late on the effects of gases on the electronic properties of carbon nanotubes (CNTs).<sup>1,2</sup> Oxygen in particular has been found to increase electrical conductance of the nanotubes, with a corresponding increase in the local density of states. The thermoelectric power is also shown to be sensitive to oxygen exposure.<sup>2</sup> While much of the recent work relates to the transport measurements of CNTs little has been done to ascertain the impact of gas exposure as it relates to field emission (FE). CNTs have shown great potential as electron field emitters due to the sharpness of their tubes, which enhances the local electric field.<sup>3–5</sup> The FE current depends strongly on the work function and geometry of the surface, and thus is susceptible to gas exposure. Previous studies have reported about the effects of gases on the FE of CNTs,<sup>6–9</sup> but these experiments were limited to a single current over a period of gas exposure. Further lacking is a comparative analysis among the various types of CNTs, such as single-walled carbon nanotubes (SWNTs) and multi-walled carbon nanotubes (MWNTs). In this letter, we present a comparative study on the effects of O<sub>2</sub>, Ar, and H<sub>2</sub> on the FE properties of SWNTs and MWNTs.

Greater than 90 wt% SWNTs were purchased from Tubes@Rice as a slurry in toluene.<sup>10</sup> The bundles had diameters of 5–20 nm and consisted of SWNTs having diameters of approximately 1.2 nm. The slurry was deposited onto a conducting Si substrate and allowed to dry. The MWNTs were prepared in our laboratory. A 150 nm layer of Fe was evaporated onto a Si substrate, which was then placed inside a tube furnace. N<sub>2</sub> at a flow rate of 250 sccm and H<sub>2</sub> at 11 sccm were introduced into the tube at a pressure of 300 Torr. The sample was then heated to 735 °C for 10 min. The H<sub>2</sub> flow was then turned off and replaced with 20 sccm of C<sub>2</sub>H<sub>2</sub> for approximately 10 min. The oven and C<sub>2</sub>H<sub>2</sub> flow were then both turned off. The N<sub>2</sub> flow rate was set at 300 sccm as the oven cooled to room temperature. The MWNTs had diameters of approximately 25 nm. To measure the FE proper-

ties of the CNTs, a positive bias was applied to a spherical platinum anode (1.1 mm diam) positioned 250 μm away to collect electrons from the grounded nanotubes.

The tunneling of electrons through a potential barrier under an applied electric field is described by the Fowler–Nordheim (FN) equation<sup>11</sup>

$$I = AV^2 \exp\left(\frac{b\phi^{3/2}}{\beta V}\right),$$

where  $I$  is the current,  $A$  and  $b$  are constants,  $\phi$  is the work function,  $V$  the applied voltage, and  $\beta$  the geometric field enhancement factor. The distance,  $d$ , between the anode and the film is an important consideration in FE analysis, therefore it is important to precisely position the anode with respect to the film. This is done using a scanning tunneling microscopy (STM) system that uses a piezoelectric inchworm motor from Burleigh Instruments.<sup>12</sup> The horizontal speed of the inchworm motor can be adjusted from approximately 2 nm/s to 0.5 mm/s. The position of the inchworm can be adjusted over 1 cm with an accuracy of  $\pm 0.25$  μm using a handset. The inchworm system is housed in an ultra-high vacuum (UHV) chamber equipped with a quadrupole mass spectrometer and UHV leak valves at a base pressure  $< 10^{-10}$  Torr. An anode and the film are loaded onto the inchworm and the sample holder, respectively, and the system is operated in STM mode. The anode slowly approaches the film until tunneling occurs at  $d \approx 0.5$ –1.0 nm. The anode is then retracted a distance of  $250 \pm 0.25$  μm from the film using the handset. Separate high-voltage electronics are used to measure the FE  $I$ – $V$  curves. Using this system, the anode can be accurately positioned for different films. In order to avoid contamination of the UHV system, the film is cleaned by heating it to 500 °C in an UHV-compatible preparation chamber for 24 h. The film is then transferred to the UHV chamber using a linear translator without exposing the film to air.

In Figs. 1, 2, and 3, the FE data are plotted  $\ln(I/V^2)$  vs  $(1/V)$  to allow comparison with the straight-line behavior predicted for FE by the FN equation. The inset in Figs. 1–3

<sup>a)</sup>Electronic mail: jperez@unt.edu

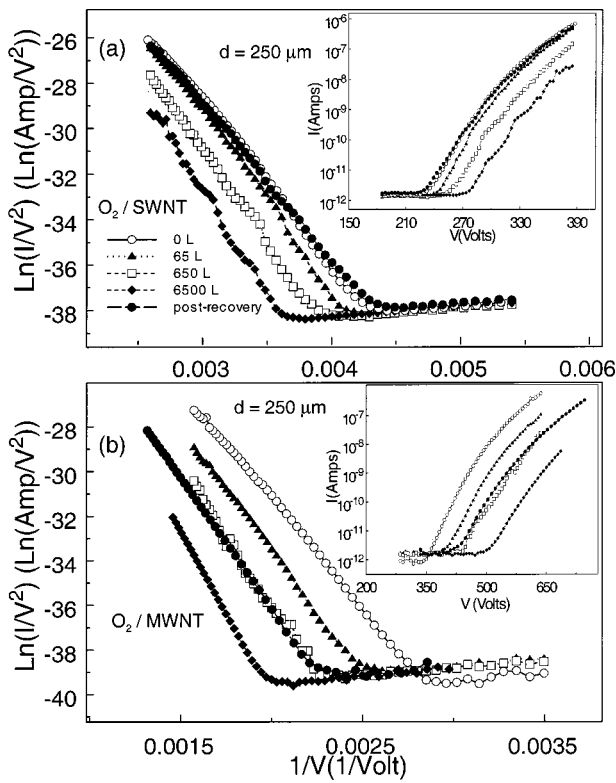


FIG. 1. Field emission plots for 0, 65, 650, and 6500 L  $\text{O}_2$  exposure of (a) single-walled carbon nanotubes and (b) multiwalled carbon nanotubes. The closed circle curves labeled postrecovery were taken last after allowing the nanotubes to operate in UHV for several hours. The inset shows a plot of the field emission current vs voltage using a log-linear scale.

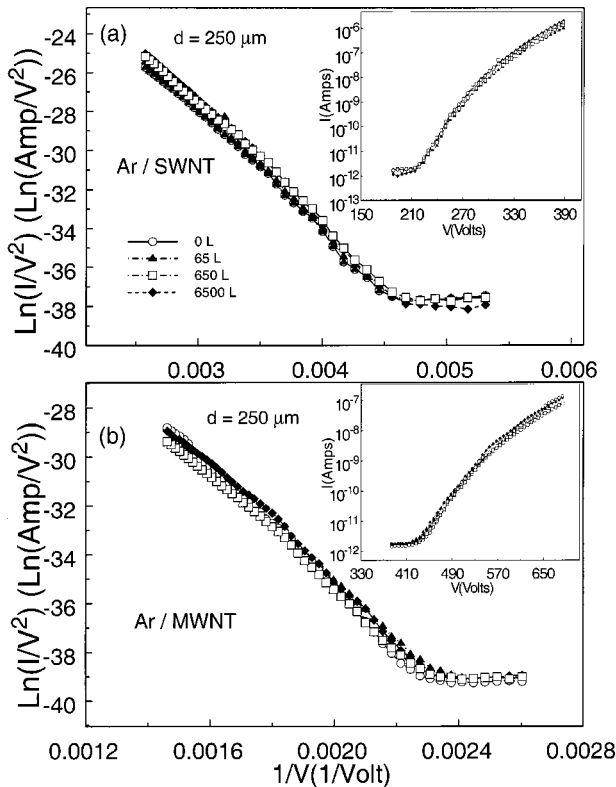


FIG. 2. Field emission plots for 0, 65, 650, and 6500 L Ar exposure of (a) single-walled carbon nanotubes and (b) multiwalled carbon nanotubes. The inset shows a plot of the field emission current vs voltage using a log-linear scale.

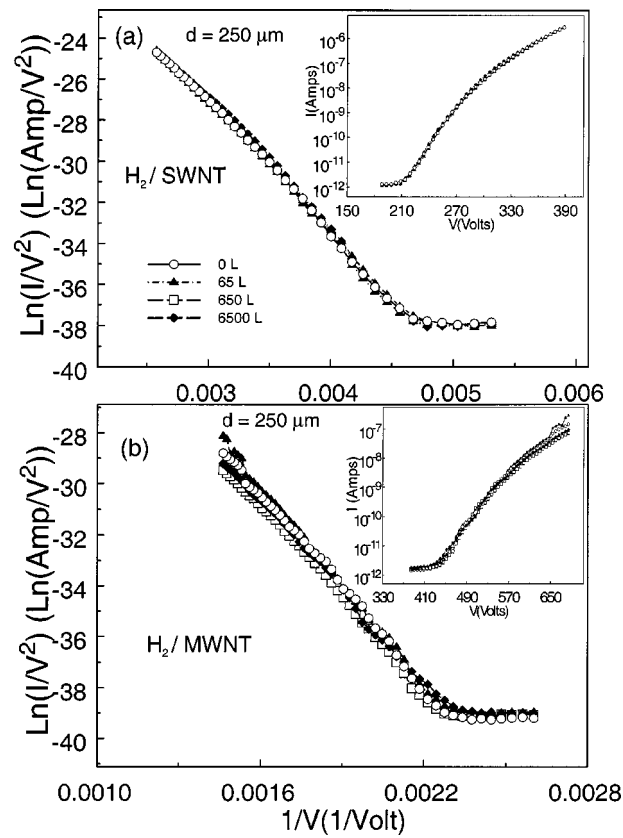


FIG. 3. Field emission plots for 0, 65, 650, and 6500 L  $\text{H}_2$  exposure of (a) single-walled carbon nanotubes and (b) multiwalled carbon nanotubes. The inset shows a plot of the field emission current vs voltage using a log-linear scale.

are the  $I-V$  curves plotted using a log-linear scale. The small current on the order of  $10^{-13}$  A observed below the threshold voltage for FE is due to leakage across the connectors. Before introducing  $\text{O}_2$ , FE  $I-V$  curves are measured in UHV, shown by the open circle plot in Fig. 1(a). To achieve approximately 65 L (1 L =  $10^{-6}$  Torr s) of exposure,  $\text{O}_2$  is leaked into the vacuum system to a pressure of  $3 \times 10^{-7}$  Torr and the nanotubes are biased at voltages that produce a FE current of  $4 \mu\text{A}$  for 216 s. These voltages are approximately 437 and 750 V for SWNTs and MWNTs, respectively. After this exposure, the vacuum system is evacuated to  $< 10^{-10}$  Torr and FE  $I-V$  curves are measured, shown by the second plot in Fig. 1(a). In this manner, the nanotubes are not exposed to  $\text{O}_2$  during the  $I-V$  curve measurement. The samples are exposed at high voltages rather than 0 V to simulate working conditions encountered in practical applications. To achieve approximately 650 L of exposure,  $\text{O}_2$  is introduced again into the vacuum chamber to a pressure of  $3 \times 10^{-7}$  Torr and the nanotubes are biased at  $4 \mu\text{A}$  for 2160 s. The voltages required are 440 and 754 V for SWNTs and MWNTs, respectively. Then the system is evacuated and the FE  $I-V$  curves are measured, shown by the plot symbolized by open boxes in Fig. 1(a). This procedure is repeated for 6500 L exposure with bias voltages of 459 and 844 V for SWNTs and MWNTs, respectively. The FE  $I-V$  curves represented by closed circles (and labeled postrecovery) were taken last after allowing the nanotubes to operate at high currents in UHV for approximately 40 h.

As shown in Fig. 1(a), introduction of  $\text{O}_2$  results in a

decrease in the FE current of SWNTs, an effect that is evident after 65 L of exposure. After 6500 L of exposure, the threshold voltage for FE has increased approximately 22% from 230 to 280 V. Before introducing O<sub>2</sub> the FE current is approximately  $5 \times 10^{-9}$  A at 300 V. After 6500 L of exposure, the FE current at 300 V decreases two orders of magnitude to about  $5 \times 10^{-11}$  A. Figure 1(b) shows the FE  $I-V$  curves of MWNTs exposed to O<sub>2</sub>. Exposure to 6500 L of O<sub>2</sub> decreases the FE current at 600 V from approximately  $2 \times 10^{-6}$  to  $2 \times 10^{-9}$  A, a decrease of three orders of magnitude. The turn-on voltage increases roughly 43% from 350 to 500 V. After allowing the emitters to run in UHV for approximately 40 h, the SWNTs recover from O<sub>2</sub> exposure as seen by the postrecovery plot in Fig. 1(a). This almost complete recovery is an indication that the initial decrease in the FE current results from a surface chemical interaction such as the formation of C–O dipoles,<sup>9</sup> and not from permanent structural damage. The dipoles likely break up and the oxygen is desorbed during the SWNTs' operation in UHV, similar to what occurs in other types of emitters such as Mo microtip arrays during field desorption cleaning.<sup>13,14</sup> The MWNTs, on the other hand, recover only up to about the second exposure as seen by the postrecovery curve in Fig. 1(b). Even after long hours (>40 h) of UHV operation at high currents (up to 10  $\mu$ A) the MWNTs showed no further improvement.

In the above experiment both SWNTs and MWNTs emit roughly the same current (4  $\mu$ A) during exposure, with the latter requiring more voltage to do so. We find that the permanent decrease in the FE current of MWNTs is bias voltage dependent. For example, exposing the MWNTs to 6500 L of O<sub>2</sub> at voltages of less than 745 V leads to full recovery of the MWNTs. Thus for MWNTs the higher electric fields may drive the oxygen ions toward enhanced surface chemical reactions, such as etching. Etching, especially at the surface caps, degrades the local geometry and can lead to a permanent decrease in the FE current.<sup>9</sup> Molybdenum arrays are known to suffer greater current degradation with increasing voltage in an oxygen environment.<sup>14</sup> In Ref. 14 this is attributed to the increased electric field and the accompanying increase in electron emission with rising voltage. SWNTs operating at FE currents up to 10  $\mu$ A and voltages up to 500 V in O<sub>2</sub> were observed to recover completely.

The FN equation shows that the value of  $b\phi^{3/2}/\beta$  can be determined from the slope of the  $\ln(I/V^2)$  vs  $I/V$  curve. From this we determined the field enhancement factor ratio  $\beta_p/\beta_0$ , where  $\beta_p$  and  $\beta_0$  are the enhancement factors for the postrecovery and 0 L curves, respectively. Our assumption was that after their long run in UHV most of the O<sub>2</sub> had desorbed off the CNTs, allowing them to recover their original work functions. Thus by taking the ratio of the slopes of the 0 L and postrecovery curves and assuming  $\phi$  is approximately the same, we measured  $\beta_p/\beta_0=1.04$  and 0.82 for SWNTs and MWNTs, respectively. This analysis is consistent with the results in Fig. 1(a) that show that the SWNTs had not suffered any structural degradation that might permanently reduce the FE current. Consistent too are the findings regarding MWNTs. The reduction in the enhancement factor is indicative of a permanent structural change having occurred, possibly from processes like etching.

Figures 2(a) and 2(b) show the FE  $I-V$  curves of SWNTs and MWNTs, respectively, after exposure to Ar. The 0, 65, 650, and 6500 L curves all roughly coincide, indicating that Ar exposure has almost no influence on the threshold voltage or FE current of CNTs. In Ref. 9 it was reported that sputtering by Ar ions does not greatly impact the FE stability of SWNTs at a single current. We find this extends to all the FE characteristics of SWNTs and MWNTs. As shown in Fig. 3(a) the 0, 65, 650, and 6500 L FE  $I-V$  curves taken after the SWNTs' exposure to H<sub>2</sub> are all approximately coincident on one another. Figure 3(b) similarly displays the results of H<sub>2</sub> exposure to MWNTs. In neither case does the impact of light hydrogen ions seem to influence the FE characteristics of the respective emitters. H<sub>2</sub> molecules are known to physisorb on the outer surfaces of CNTs as well as in between the interstitial spaces separating the CNTs.<sup>15,16</sup> Their easy desorption in a high field environment may explain the lack of influence of H<sub>2</sub> molecules on the FE characteristics of CNTs.

In summary, O<sub>2</sub> exposure temporarily increases the turn-on field of SWNTs by 22% and decreases the FE by two orders of magnitude. However, the FE properties completely recover after approximately 40 h of FE operation in UHV. For MWNTs, the higher voltage O<sub>2</sub> exposure leads to a 43% increase of the turn-on field and reduction of FE current by three orders of magnitude. The recovery in UHV is only partial, indicating that the MWNTs suffer permanent degradation of their FE characteristics. The ratios of the slopes before and after O<sub>2</sub> exposure are approximately 1.04 and 0.82 for SWNTs and MWNTs, respectively, indicating that the geometric field enhancement factor of MWNTs decreases after O<sub>2</sub> exposure. H<sub>2</sub> and Ar gases do not significantly affect the FE properties of SWNTs or MWNTs.

This work was supported, in part, by the National Science Foundation under Award No. DMR-0074636 and by the Texas Advanced Technology Program under Award No. 003594-0048-1999.

<sup>1</sup>J. Kong, N. R. Franklin, C. Zhou, M. G. Chapline, S. Peng, K. Cho, and H. Dai, *Science* **287**, 622 (2000).

<sup>2</sup>P. G. Collins, K. Bradely, M. Ishigami, and A. Zettl, *Science* **287**, 1801 (2000).

<sup>3</sup>A. G. Rinzler, J. H. Hafner, P. Nikolaev, L. Lou, S. G. Kim, D. Tomaneck, P. Nordlander, D. T. Nordlander, D. T. Colbert, and R. E. Smalley, *Science* **269**, 1550 (1995).

<sup>4</sup>W. A. de Heer, A. Chatelain, and D. Ugarte, *Science* **270**, 1179 (1995).

<sup>5</sup>J. M. Macaulay, I. Brodie, C. A. Spindt, and C. E. Holland, *Appl. Phys. Lett.* **61**, 997 (1992).

<sup>6</sup>J.-M. Bonard, J.-P. Salvetat, T. Stockli, and W. A. de Heer, *Appl. Phys. Lett.* **73**, 918 (1998).

<sup>7</sup>J.-M. Bonard, F. Maier, T. Stockli, A. Chatelain, W. A. de Heer, J.-P. Salvetat, and L. Forro, *Ultramicroscopy* **73**, 7 (1998).

<sup>8</sup>D. S. Chung *et al.*, *J. Vac. Sci. Technol. B* **18**, 1054 (2000).

<sup>9</sup>K. A. Dean and B. R. Chalamala, *Appl. Phys. Lett.* **75**, 3017 (1999).

<sup>10</sup>Tubes@Rice, P.O. Box 1892, Houston, TX 77251.

<sup>11</sup>R. H. Fowler and L. Nordheim, *Proc. R. Soc. London, Ser. A* **119**, 683 (1928).

<sup>12</sup>Burleigh Instruments, Inc., Fishers, NY 14453.

<sup>13</sup>E. W. Mueller and T. T. Tsong, *Field Ion Microscopy, Principles and Applications* (Elsevier, New York, 1969).

<sup>14</sup>B. R. Chalamala, R. M. Wallace, and B. E. Gnade, *J. Vac. Sci. Technol. B* **16**, 2859 (1998).

<sup>15</sup>Y. Ye, C. C. Ahn, C. Witham, B. Fultz, J. Liu, A. G. Rinzler, D. Colbert, K. A. Smith, and R. E. Smalley, *Appl. Phys. Lett.* **74**, 2307 (1999).

<sup>16</sup>A. C. Dillon, K. M. Jones, T. A. Bekkedahl, C. H. Kiang, D. S. Bethune, and M. J. Heben, *Nature (London)* **386**, 377 (1997).